UDC 539.4

Fracture Process in $\pm\theta$ Laminates Subjected to Mode II Loading

A. Ahmed Benyahia,[a] A. Laksimi,[a] S. Benmedakhene,[a] and X. L. Gong[b]

[a] Laboratoire Roberval UMR-CNRS-6066 Université de Technologie de Compiègne (UTC), Compiègne, France

[b] LASMIS, GSM, Université de Technologie de Troyes (UTT), Troyes, France

УДК

Процесс разрушения в $\pm\theta$-ламинатах, подвергнутых нагружению по типу K_{II}

А. Ахмед Беньяхья[а], А. Лаксими[а], С. Бенмедахен[а], Кс. Л. Гонг[б]

[а] Технологический университет, Компьень, Франция

[б] Технологический университет, Труа, Франция

Исследуется поведение многомерного ламината при его нагружении по типу K_{II}. Описан процесс деламинирования упрочненного стеклоэпоксидного композита. Для минимизации эффектов трения выбрана ориентация $\pm\theta$. Рассмотрена методика межламинарных испытаний по типу K_{II} с использованием схем трехточечного и консольного изгиба соответственно образцов типа ENF (торцевое защемление с консольным изгибом нагрузкой, равномерно распределенной по ширине свободного торца) и ELS (шарнирно закрепленная балка с центральной нагрузкой, равномерно распределенной по ширине балки). Представлены экспериментальные методики и результаты исследования скоростей высвобождения энергии деформации при инициировании трещин. Для двух вышеуказанных типов образцов проанализирован процесс разрушения и механического поведения материала. Установлена тесная корреляционная связь между величинами угла θ, соотношением a/L и толщиной образцов h. Показано, что разрушение вследствие деламинации возможно только при условии оптимального выбора этих параметров. Анализ напряженного состояния в вершине трещины позволяет объяснить явление межслойной бифуркации, его результаты хорошо согласуются с экспериментальными данными.

Ключевые слова: $\pm\theta$-ламинаты, нагружение по II типу, деламинирование, бифуркация, процесс разрушения, анализ напряженного состояния.

Introduction. The last 20 years have seen the development of a very extensive range of tests designed to quantify the toughness of continuous fiber–reinforced composites.

These tests are generally identified by the type of loading applied as Mode I, Mode II, Mode III, or Mixed mode.

Delamination tests under bending conditions have been usually performed on unidirectionally reinforced fiber composites [0°] in order to determine interlaminar fracture resistance G_{IIc}.

However, the structure of fiber-reinforced composites commonly used in industry is made of stratified layers of the type $[\pm\theta]$. Initial defects from the

manufacture process can be located anywhere in a multidirectional laminate, and during loading, these defects can propagate and lead to complete fracture. In such materials, the presence of an interlaminar defect divides the composite into two sections, analogous to the two arms of a double cantilever beam (DCB) specimen, whose mechanical behavior must be well defined. This mechanical behavior depends essentially on the plies orientation. Analysis of the stress and strain fields around the crack tip, as well as the fracture mechanisms become more complex than those in unidirectional composite structures.

Moreover, comparison is made between the values of the energy release rate for various interfaces without taking account the stacking sequences. When a crack propagates at large angles (especially [90°]), the strain-energy release rate is dissipated not only during initiation and propagation of delamination but also in the nucleation of transverse cracks in these plies. This phenomenon, which is called bifurcation, is due to the edge effect [1–2]. Few studies concern the Mode II cases because of the difficulties encountered when using the concept of the linear elastic fracture mechanic (LEFM) to obtain the energy release rate G_{II}.

The study of Mode II in the case of laminates $\pm\theta$ requires preliminary adaptation of specimen dimensions according to the used angle θ. The difficulties in designing a Mode II specimen is to avoid any cracking by opening without causing an excessive friction between the two faces of the crack.

In order to characterize the Mode II, three-point bending and cantilever flexure tests [ENF (End Notch Flexure) and ELS (End Load Split)], respectively, are used. However, the specimen geometry must take into account the length L, the thickness h, and the crack length a. It must be noted that certain composite materials like glass-epoxy, which have a rather low Young's modulus due to a significant length L, exhibit large displacement before the beginning of delamination. The aim of this study is to get a better understanding of the behavior of multidirectional composites, which depends on the orientation of plies, stacking sequences, and crack location under Mode II loading.

1. **Experimental Analysis**.

1.1. **Material and Experimental Procedures**. The material used in this study is an E-glass/M10-epoxy composite. The fiber volume fraction is about 52%. Test specimens were cut from plates of size 300 × 300 mm. A Teflon film (30 μm in thickness) was incorporated at the mid-plane to initiate delamination (Fig. 1). The thickness of 4.8 mm is composed of 16 plies. The plates were cured in an air press according to the cure cycle recommended by the manufacturer (3 bars for 1 hour at 120°C). Four configurations $[(+\theta/-\theta)_{2s}]_s$ were selected with the angles: $\theta = 15°$, 30°, 45°, and 60°.The starter film was inserted in the interface between θ/θ laminate at the mid-plane of the stacking sequence: $(+\theta/-\theta/+\theta/-\theta/-\theta/+\theta/-\theta/+\theta//+\theta/-\theta/+\theta/-\theta/-\theta/+\theta/-\theta/+\theta)$. In order to study the shearing mode, two types of specimens (ELS and ENF) were used (Fig. 1), whose dimensions are shown in Table 1.

Each specimen was instrumented with an acoustic emission transducer and strain gauges were placed on the specimen surfaces as indicated in Fig. 1. The specimens were loaded with displacement control at a constant rate of 0.5 mm/min in order to observe better the occurrence of damage mechanisms.

Table 1

Geometrical Characteristics of ELS and ENF Specimens

Specimens	Width B, mm	Length L, mm	Total thickness $2h$, mm	Ratio a_0/L
ELS	20	60	4.8	$0.4 < a_0/L < 0.7$
ENF	20	50	4.8	$0.4 < a_0/L < 0.7$

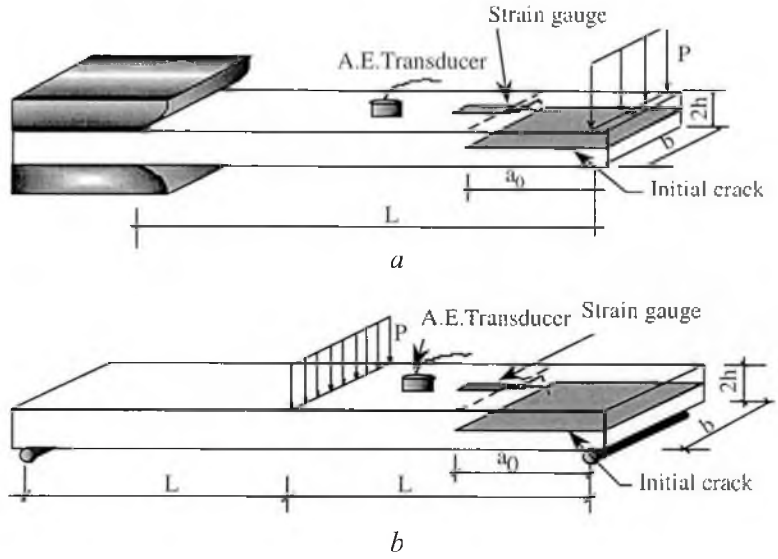

Fig. 1. ELS (*a*) and ENF (*b*) specimens.

1.2. **Data-Reduction Method**. The mechanical approach involves determination of the energy release rate by the compliance method:

$$G_{\mathrm{II}} = \frac{P^2 \partial c}{2B\partial a}. \tag{1}$$

Here, P is the applied load, B is the specimen width, and $\dfrac{\partial c}{\partial a}$ is the partial derivative of the compliance with respect to the crack length. Four specimens were tested for each laminate.

The calibration of compliance was made according to the rule $c = \alpha + \beta a^3$ [3], where α and β are material parameters determined for various ratios a_0/L. The values obtained for four configurations are summarized in Table 2.

The results for the energy release rate $G_{\mathrm{II}\max}$ corresponding to the maximum load $P_{\max}$ are summarized in Table 3.

The $G_{\mathrm{II}\max}$ values corresponding to the sequence $\theta = \pm 60°$ could not be given because of the specimen fracture by flexure without delamination. All the configurations seem to have fracture energies ($G_{\mathrm{II}\max}$), which converge towards a value of approximately 2 kJ/m^2.

Table 2

Compliance Parameters α and β Depending on θ

Laminate	±15°	±30°	±45°	±60°
$\alpha \cdot 10^{-2}$, mm/N	1.42	2.21	1.80	2.36
$\beta \cdot 10^{-7}$, $(\text{N} \cdot \text{mm}^2)^{-1}$	1.55	1.85	3.56	7.10

Table 3

Energy Release Rate for ELS Specimen

Sequences θ, deg	a_0/L	$G_{\text{II max}}$, kJ/m^2
0	0.4	2.63 (0.28)
	0.5	2.43 (0.21)
	0.6	2.45 (0.19)
±15	0.4	1.91 (0.13)
	0.5	2.07 (0.14)
	0.6	1.99 (0.15)
	0.7	2.13 (0.12)
±30	0.4	1.51 (0.09)
	0.5	1.96 (0.12)
	0.6	2.10 (0.08)
	0.7	1.89 (0.08)
±45	0.4	0.92 (0.04)
	0.5	1.51 (0.08)
	0.6	1.38 (0.08)
	0.7	1.16 (0.06)

Note. Here and in Table 4 in parentheses are given standard deviations.

Table 4

Energy Release Rate for ENF Specimen

Sequences θ, deg	a/L	G_{IIc}, kJ/m^2
15	0.4	1.380 (0.25)
	0.5	1.560 (0.20)
	0.6	2.060 (0.21)
	0.7	2.043 (0.22)
30	0.4	1.360 (0.13)
	0.5	1.680 (0.14)
	0.6	1.917 (0.13)
	0.7	1.927 (0.12)
45	0.4	1.520 (0.09)
	0.5	1.240 (0.09)
	0.6	1.550 (0.07)
	0.7	1.660 (0.08)

The absence of the $G_{\text{II max}}$ values for the sequence $\pm 60°$ in Table 4 is due to the fact that this sequence practically does not have delamination, except for the ratios a_0/L that is very close to unity, and the stress field at the tip of the initial crack is completely modified. It appears that before delamination composites $[\pm\theta]$ subjected to Mode II loading by flexure have highly scattered

damages especially by transverse cracks. A transverse crack is perpendicular to the direction of propagation, it cannot be assimilated to a pseudo-length of the crack as required by the LEFM concepts.

Transverse cracks are responsible for the significant nonlinearity especially for large angles.

The strain energy release rate $G_{\text{II}\max}$ for large angles (> 17°) remains well below 2.5 kJ/m^2 that represents the intrinsic resistance to delamination of the material used in this study. This means that delamination is always preceded by transverse cracks, which generate significant shear stresses ahead of the crack tip.

From the above observations it appears that the behavior of the angle-ply laminates is more complex than that of unidirectional materials. The phenomenon of bleaching (damage of glass-matrix appears as a whitening aspect) and the specimen low stiffness involve large displacements and nonlinear behavior, which may invalidate the fracture mechanics concepts. These remarks determine optimization of the specimen dimensions as it is discussed below.

2. **Specimen Optimization**. The use of the concepts of the linear elastic fracture mechanics is valid only in the case of the linear elastic behavior with small displacements. Their application requires a check on two behavior conditions in order:

– to avoid nonlinearity resulting from large displacements,

– to avoid nonlinearity of the material or fracture by flexure.

On this subject, Carlsson et al. [4] presented the analysis based on the beam theory that allows the calculation of dimensions for an ENF specimen.

The first condition results in a maximum value of the slope y'_a, at the loading point.

The acceptable displacement (δ_a) corresponding to y'_a can be calculated from Eq. (2):

$$\frac{dy}{dx} = \frac{3(L^2 + 3a^2)\delta}{2L^3 + 3a^3}. \tag{2}$$

The critical displacement of fracture initiation is given by the following relation:

$$\delta_c = \frac{2L^3 + 3a^3}{6a}\sqrt{\frac{G_{\text{II}c}}{E_1 h^3}}. \tag{3}$$

The condition $\delta_c \le \delta_a$ allows us to optimize the specimen dimensions by combining Eqs. (2) and (3). For example, if the thickness h is the parameter, which controls the specimen behavior, we have:

$$h \ge \sqrt{\frac{G_{\text{II}c}(L^2 + 3a^2)^2}{4(y'_a)^2 a^2 E_1}}, \tag{4}$$

where $G_{\text{II}\max}$ is the energy of the crack propagation initiation, L is the half-length of the specimen, a is the initial crack length, and E_1 is the flexure modulus in the longitudinal direction.

For the second condition, optimization will be made according to the permissible flexure strain. For the ratio $a/L < 0.5$, if there is fracture by flexure, it occurs in the median section between the supports, where the maximum strain is given by

$$\varepsilon_m = \frac{6Lh\delta}{2L^3 + 3a^3}. \tag{5}$$

In the same way as for the first condition, the optimization of the thickness gives

$$h \geq \frac{L^2 G_{IIc}}{a^2 \varepsilon_{ma}^2 E_1}, \tag{6}$$

where ε_{ma} is the permissible flexure strain.

The study by the finite elements realized by Mall and Kochhar [5] showed that the linear elastic analysis can be used if the critical displacement does not exceed the total thickness of the specimen 1.5 times $[\delta \leq \frac{3}{2}(2h)]$, otherwise the G_{II} value will be overestimated.

In the same way as for the ENF specimen, it is possible to use the nonlinearity conditions for ELS specimens used in this study. In the case of nonlinearity due to large displacements, an acceptable displacement (δ_a) can be calculated by Eq. (7) for an acceptable slope y'_a:

$$\frac{dy}{dx} = \frac{3(3a^2 + L^2)}{2(3a^3 + L^3)}\delta. \tag{7}$$

The starting critical displacement is given by relation (8):

$$\delta_c = \frac{L^3 + 3a^3}{3a}\sqrt{\frac{G_{IIc}}{E_1 h^3}}. \tag{8}$$

On combining Eqs. (7) and (8), the condition $\delta_z \leq \delta_a$ allows us to optimize the thickness (h) with relation (9):

$$h \geq \sqrt[3]{\frac{G_{IIc}(L^2 + 3a^2)^2}{4(y'_a)^2 a^2 E_1}}. \tag{9}$$

In the case of nonlinearity due to fracture by flexure, optimization is to be done according to the acceptable strain of fracture by flexure. For the ratio $a/L < 0.5$, if there is fracture by flexure, it occurs on the cantilever, where the strain is maximal and is given by

$$\varepsilon_m = \frac{3Lh\delta}{L^3 + 3a^3}. \tag{10}$$

Fracture by flexure can be avoided using the optimum thickness h. This is the same relation as for the ENF specimen:

$$h \geq \frac{L^2 G_{\mathrm{II}c}}{a^2 \varepsilon_{ma}^2 E_1}. \tag{11}$$

Thus, the optimization by the application of the nonlinearity conditions requires the knowledge of the following parameters: $G_{\mathrm{II}\max}$ (the energy-release rate in Mode II), ε_{ma} (fracture strain of the material), and E_1 (the longitudinal modulus of elasticity obtained by flexure). It should be noted that only $G_{\mathrm{II}\max}$ (2.5 kJ/m^2) is intrinsic to the laminate material whatever the orientation angle of the plies. On the other hand, ε_{ma} and E_1 depend on the orientation of the plies and their values are summarized in Table 5. The ε_{ma} values are calculated by the application of the interactive criterion of Tsai [6]. As for the E_1 values, they are determined by the laminate theory.

Table 5

Mechanical and Energy Characteristics for Various Sequences

Sequences θ, deg	E_1, GPa	$\varepsilon_{ma} \cdot 10^{-3}$	$G_{\mathrm{II}c}$, kJ/m^2 (average)
0 (unidirectional)	44.110	24.55	2.5
±15	38.560	9.95	
±30	26.939	6.20	
±45	18.354	4.00	
±60	16.432	2.53	

A numerical simulation for a unidirectional laminate in this study with $G_{\mathrm{II}\max} = 2.5$ kJ/m^2, $\varepsilon_{ma} = 24.55 \cdot 10^{-3}$, $E_1 = 44{,}110$ MPa, $h = 2.4$ mm, $\delta_c = 3h$, and $a_0/L = 0.5$ has given the following specimen lengths:

$L \leq 67$ mm for the first condition of nonlinearity (large displacements);

$L \leq 42$ mm for the second condition of nonlinearity (fracture by flexure).

The second condition of nonlinearity proves to be more severe and should be used for any optimization. The length $L = 40$ mm appears to be very practical in the case of the ENF specimen whose total length is 80 mm. However, in the case of the ELS specimen, this length is insufficient because of the resistance of the assembly. It should also be noted that this length was calculated for a unidirectional laminate. Consequently, the application of the same condition to laminates $\pm\theta$ (with $\theta > 0°$) certainly requires lower lengths (L).

The application of Eq. (11) allows us to determine, for the thickness h and a given ratio a/L, the minimum strain em that causes fracture by delamination. Thus, as long as $\varepsilon_m < \varepsilon_{ma}$, fracture occurs completely by delamination. On the

other hand, if $\varepsilon_m >> \varepsilon_{ma}$, fracture occurs completely by flexure. As for the cases where ε_m is higher but very near to ε_{ma}, the process of fracture is the combination of fractures by flexure and delamination. In fact, in this intermediate case, the initiation of fracture is caused by flexure (transverse fracture of the first ply, which is extremely stretched), then delamination occurs under the effect of increasing shear stresses due to fracture of the first ply. This calculation and checking procedure must be carried out for all the stacking sequences and for the ratio a/L growing from 0 to 1.

However, if for $a/L < 0.5$, the maximum strain is at the point m (Fig. 2), for $a/L > 0.5$, the maximum strain is at the tip of the initial crack (point t). The relation between the two strains at the points m and t is treated by the conventional theory of beams.

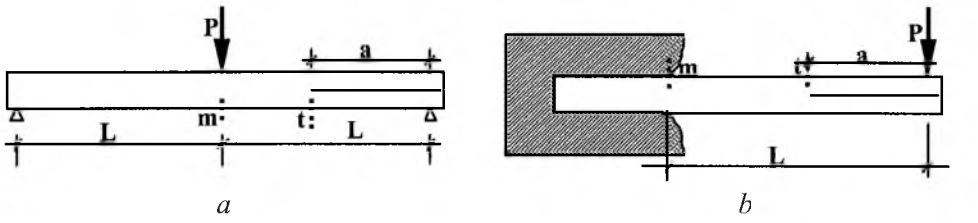

a *b*

Fig. 2. Dangerous sections in ENF (*a*) and ELS (*b*) specimens.

In this case, the stresses at the points m and t are given by the following relations:

$$\sigma_m = \frac{3PL}{4bh^2} \quad \text{and} \quad \sigma_t = \frac{3Pa}{2bh^2} \quad \text{for an ENF specimen,}$$

$$\sigma_m = \frac{3PL}{2bh^2} \quad \text{and} \quad \sigma_t = \frac{3Pa}{bh^2} \quad \text{for an ELS specimen.}$$

Therefore, $\sigma_t = \frac{2a}{L}\sigma_m$ for the two specimen types and arbitrary ratio a/L.

Consequently, for the two specimen types $\varepsilon_t = \frac{2a}{L}\varepsilon_m$.

Thus, for any ratio $a/L < 0.5$ and $\varepsilon_t < \varepsilon_m$, a check for fracture by flexure must be carried out at the point m, where the section is more dangerous. On the other hand, for any ratio $a/L > 0.5$ and $\varepsilon_t > \varepsilon_m$, the check for fracture by flexure is done at the point t.

The minimum values of ε_m (for $a/L < 0.5$) and ε_t (for $a/L > 0.5$), which cause fracture by delamination, for the thickness $h = 2.4$ mm are presented in Table 6. It is necessary to note that for the ratio $a/L = 0$, the strain ε_m is infinite. That means that for this ratio ($a/L = 0$) the specimen does not contain any initial crack and the initiation of fracture occurs by flexure at the point m without the risk of delamination in the median plane of the specimen end.

The value of ε_m decreases with increasing ratio a/L and increases with the orientation angle of the plies. However, when $a/L > 0.5$, although the strain ε_m continues to decrease with an increase in the ratio a/L, the strain ε_t remains

constant. Its values correspond to the ratio $a/L = 0.5$ and remain constant at $a/L \geq 0.5$.

A comparison between the minimum strains ensuring fracture by delamination and the fracture strains in flexure is made in Table 6. It is clear that fracture initiation is always caused by flexure in the following cases (see Fig. 3):

– for the ratio $a/L < 0.2$ and any orientation angle of the plies (even for a unidirectional composite);

– for all $\theta \geq 15°$ and any ratio a/L.

T a b l e 6

Minimum Strains Ensuring Fracture by Delamination

Sequences θ, deg	$\varepsilon_m \cdot 10^{-3}$					$\varepsilon_t \cdot 10^{-3}$
	$a/L = 0$	$a/L = 0.2$	$a/L = 0.3$	$a/L = 0.4$	$a/L = 0.5$	$a/L > 0.5$
0	∞	24.55	16.20	12.10	9.72	9.72
±15	∞	25.60	17.32	12.99	10.40	10.40
±30	∞	31.10	20.73	15.54	12.00	12.00
±45	∞	37.66	25.11	18.83	15.06	15.06
±60	∞	39.81	26.54	19.90	15.90	15.90

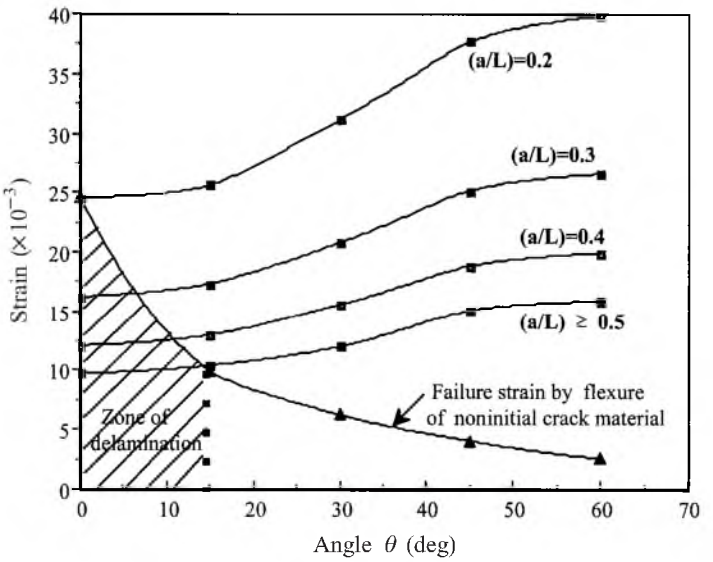

Fig. 3. A graph giving fracture strains in flexure according to the orientation angle θ of the plies and the a/L ratio.

As for fracture by delamination, it occurs when the conditions of the angle θ and the ratio a/L are limited by the contour of the shaded zone. In fact, when θ is lower than 15°, any couple (θ, and a/L), which is below the curve of failure strain by flexure for undamaged material, causes delamination without transverse cracking. For example, for $\theta = 10°$, all the ratios $a/L \geq 0.4$ cause fracture by delamination alone (without transverse cracking).

The same remark can be made for the optimization of the specimen thickness. To this effect, the application of Eq. (6) allows us to determine, for a given fracture strain by flexure and a given ratio a/L, the necessary minimum thickness to ensure fracture by delamination. Table 7 summarizes the minimum values of the thickness h necessary for all the sequences of stratification and the ratio a/L from 0 to 1. A comparison between these results and the real thickness of the material in this study is illustrated in Fig. 4. The analysis of various curves in this figure makes it possible to explain the fracture process in $\pm\theta$ laminates according to the specimen thickness and the ratio a/L.

Table 7

The Minimum Thickness Values Ensuring Fracture by Delamination

Sequences θ, deg	Half-thickness of the specimens				
	$a/L = 0$	$a/L = 0.2$	$a/L = 0.3$	$a/L = 0.4$	$a/L = 0.5$
0l	∞	2.30	1.04	0.58	0.38
±15	∞	16.37	7.27	4.10	2.62
±30	∞	60.00	26.82	15.09	9.65
±45	∞	212.00	94.60	53.20	34.05

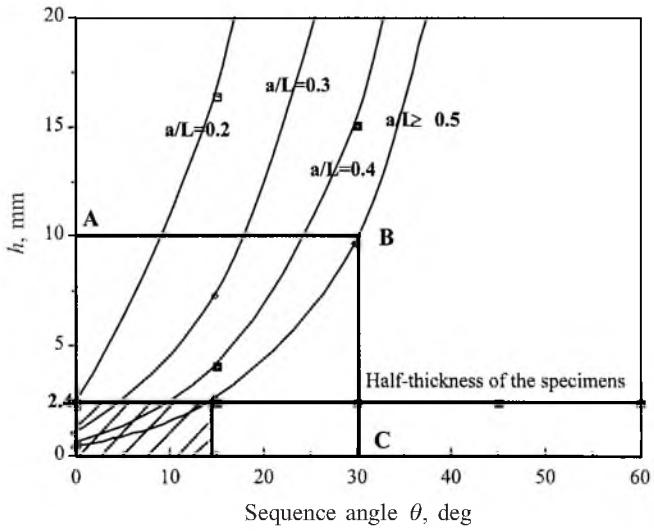

Fig. 4. The minimum thickness ensuring fracture by delamination.

We can clearly see a close relation between the angle θ, the ratio a/L, and the thickness h of the material. Fracture by delamination can be obtained only with an optimum choice among these three parameters. For example, for $\theta = 20°$ associated with the ratio $a/L = 0.4$, the adequate thickness h to cause fracture by delamination is lower or equal to 0.6 mm, whereas it can almost double for the ratio $a/L = 0.3$.

As for the material in this study ($h = 2.4$ mm), fracture takes place by simple delamination for any couple (θ, a/L) pertaining to the small hatched rectangle

(Fig. 4). Thus, for all the sequences studied, fracture cannot occur only by delamination if the specimens are loaded in Mode II by flexure that was checked by experiments. It is easy to see that microcracks generated by flexure in Mode II grow by coalescence and lead to the bifurcation phenomenon, especially in the adjacent delamination plies. This damage process becomes more important and takes place in the plies having a large angle θ. This damage mechanism occurs even in Mode I [6, 7]. But the question is how this bifurcation phenomenon appears around the crack tip in this case, and what types of stresses are involved in this mechanism. In order to have a better understanding of the appearance of transverse cracks in this case, analysis of the fracture process at the crack tip is presented.

3. **Analysis of the Fracture Process in ENF and ELS Specimens**. The results of optimization of ENF and ELS specimens allow us to identify 3 modes of fracture: fracture by delamination alone, transverse fracture only by flexure, and fracture by the combination of the last two modes.

With regard to the first mode, fracture by delamination alone is present in two types of laminates (unidirectional and multidirectional ($\pm\theta$)) for which the couple (θ, a/L) is inside the small hatched area of Fig. (3). The delamination propagation occurs at the median interface ($+\theta/+\theta$). This fracture mode can be explained in two ways:

– the material toughness in Mode II (2.5 kJ/m^2) is lower than the work of the external forces necessary to cause fracture by flexure;

– the ratio of the shear stress at the crack tip (τ_t) to the fracture shear stress (τ_R) is much larger than the ratio of the maximum flexure stress (σ_{mf}) to the fracture stress (σ_{Rf}) by flexure ($\tau_t/\tau_R >> \sigma_{mf}/\sigma_{Rf}$).

For the second mode, fracture by flexure alone occurs for the values of (θ, a/L) very far from the rectangle $OABC$ (Fig. 4). It is necessary that the distance of the (θ, a/L) values from the rectangle $OABC$ be such that the amplification of the shear stress after failure of the first ply could not generate delamination. For example, for the practical ratio $a/L \geq 0.5$ (the ratio that allows a stable propagation), all the laminates ($\pm\theta$) for which $\theta > 60°$ fracture only by flexure.

The third mode characterized by both delamination and fracture by flexure is more complex and requires a particular study. Indeed, in this case, fracture is initiated by transverse cracks within two extremely stressed plies ($+\theta$) causing a transfer of delamination towards the interface ($+\theta/-\theta$) to a ply of the median plane. For better understanding of this mode of delamination plane, it would be necessary to analyze the distribution of stresses surrounding the tip of the initial crack.

However, the majority of works treating stress distributions in fractured laminates concern the sequences loaded under simple tension and necessarily containing plies oriented at 90°. Having the weakest ultimate deformation, the plies oriented at 90° are the best case for studying transverse cracking. The basic methods of calculation developed for the stress distribution analysis are:

– shear-lag method;
– variational approach;
– theory of internal variables;
– statistical approach.

In this study, the shear-lag method is adopted for the analysis of stress distribution, which is studied around the tip of the initial crack. In fact, the most dangerous section under the effect of flexure is located at the tip of the initial crack, where $a/L \geq 0.5$ (stable propagation). In the elastic linear phase, the stress field surrounding the tip of the initial crack is presented in Fig. 5.

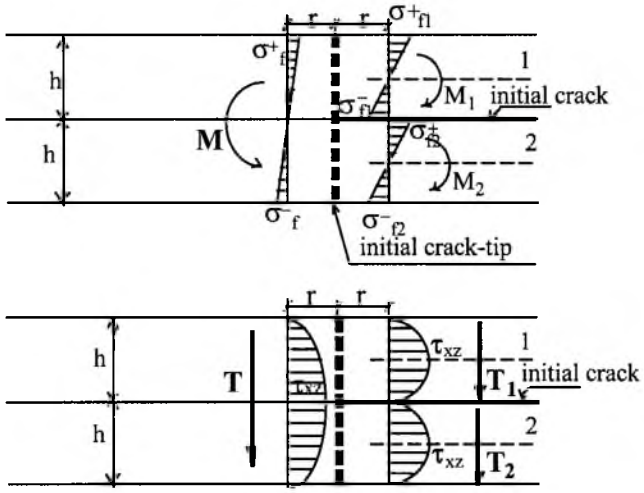

Fig. 5. Flexure and shear stress fields in the vicinity of the initial crack tip at the elastic phase.

When the bending stress reaches the limiting value $\tilde{\sigma}_{f\theta}$ within the stretched median ply $(+\theta)$, a transverse crack is initiated on its right side at the tip of the initial crack. At this crack, the neutral axis moves from (A.N.1) towards (A.N.2) (Fig. 6) annulling the bending stress. The remaining part of the specimen's arm section has a new stress distribution. The evolution of the neutral axis and of the new distribution of bending stresses around the transverse crack is illustrated in Fig. 6. While moving away from the crack, the bending stress $\sigma_f(x)$ in the failure ply increases exponentially until reaching the maximum whose value remains somewhat lower than $\tilde{\sigma}_{f\theta}$.

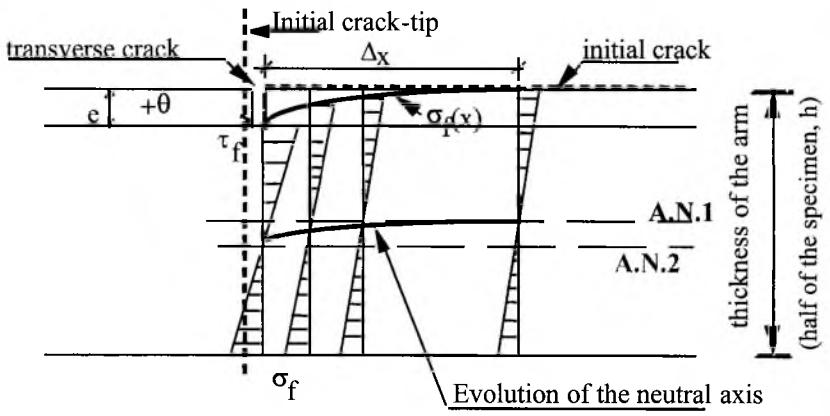

Fig. 6. Redistribution of bending stresses and evolution of the neutral axis near a transverse crack.

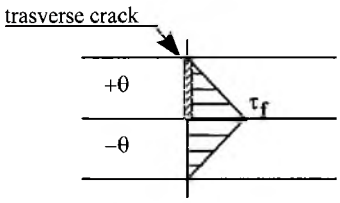

Fig. 7. Appearance and distribution of shear stresses near a transverse crack due to flexure.

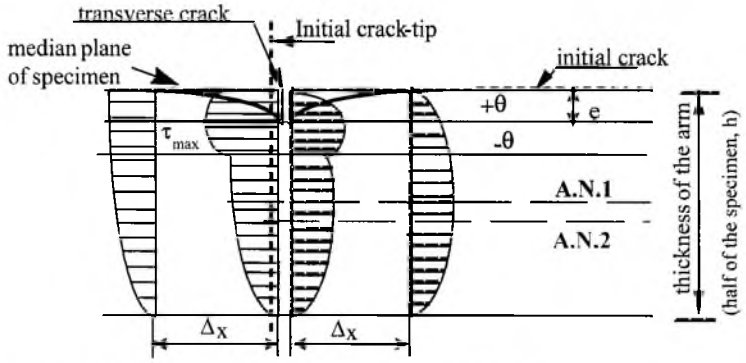

Fig. 8. Redistribution of shear stresses near a transverse crack.

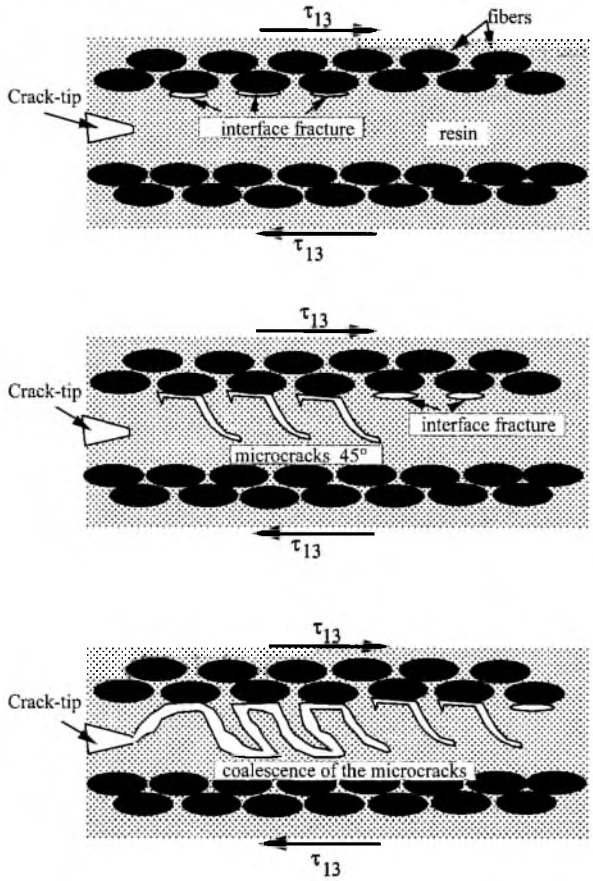

Fig. 9. Scheme of the crack propagation process in the ± θ laminate loaded under Mode II conditions.

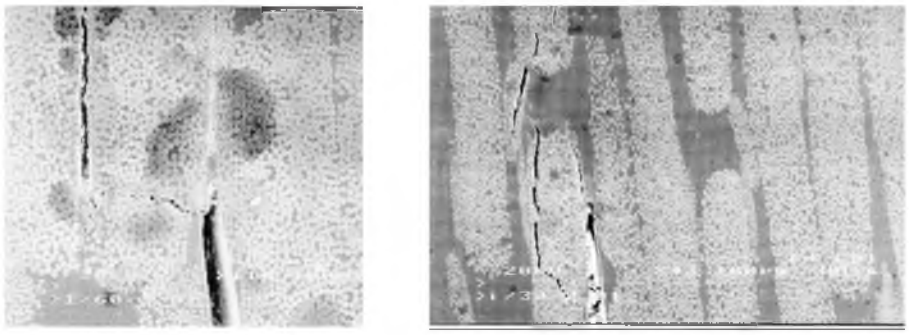

a *b*

Fig. 10. Crack bifurcation at the crack tip: (a) crack initiation, (b) crack propagation.

Fig. 11. Coalescence of microcracks.

However, because of the transverse crack, the bending stress is transformed into the shear stress (τ_f) and then becomes an additional stress to the remaining part of the section. As the shear modulus is the same for the plies $+\theta$ and $-\theta$, the new shear stress τ_f is distributed through the thickness on both sides of the interface ($+\theta$) and ($-\theta$) (Fig. 7). The effect of the shear stress τ_f on the continuation of the fracture mode is decisive. Indeed, the stress τ_f added to the stress τ prior to bifurcation causes redistribution of the shear stress (Fig. 8). This successive redistribution of the shear stress is the cause of the stepwise crack propagation. Consequently, the dangerous zone under the effect of shear is the interface $+\theta/-\theta$ toward the adjacent ply of the median plane. Thus, the delamination expected on the median interface $+\theta/+\theta$ is transferred towards the interface $+\theta/-\theta$.

In any case, according to observations of Purslow [9], the evolution of delamination in Mode II occurs as shown in Figs. 9 and 10. Fracture initiation takes place at the matrix-fiber interface and the coalescence occurs by forming strips at 45° according to shearing fracture (Fig. 11).

Conclusions. The angle of orientation θ has a significant influence on the value of the energy release rate G_{IIc}.

The Mode II tests on ENF and ELS specimens with angles $\pm\theta$ require a preliminary geometrical optimization in order to avoid transverse cracking apart from the median plane, which dissipates energy. This study shows the existence of

a close relation between the angle θ, the ratio a/L, and the thickness h of the material. For the 5-mm thickness and the sequences of stratification studied, fracture cannot occur by delamination only without transverse cracking.

The analysis of the stress state at the crack tip allows us to explain the phenomenon of bifurcation between plies and it is in good agreement with the experimental results. A successive redistribution of the shear stresses is the main cause of bifurcation and stepwise crack propagation.

Fracture initiation takes place at the matrix–fiber interface and the coalescence occurs by the formation of strips at 45° according to fracture by shear.

Резюме

Досліджується поведінка багатовимірного ламіната при його навантаженні за типом K_{II}. Описано процес деламінування зміцненого склоепоксидного композита. Для мінімізації ефектів тертя вибрано орієнтацію $\pm\theta$. Розглянуто методику міжламінарних випробувань за типом K_{II} із використанням схем триточкового і консольного згину відповідно зразків типу ENF (торцеве затиснення з консольним згином навантаженням, що рівномірно розподілене по ширині вільного торця) і ELS (шарнірно закріплена балка з центральним навантаженням, що рівномірно розподілене по ширині балкі). Представлено експериментальні методики і результати щодо швидкостей звільнення енергії деформації при ініціюванні тріщин. Для двох вищевказаних типів зразків проаналізовано процес руйнування і механічної проведінки матеріалу. Установлено кореляційний зв'язок між величинами кута θ, відношенням a/L і товщиною зразків h. Показано, що руйнування внаслідок деламінації можливе лише за умови оптимального вибору цих параметрів. Аналіз напруженого стану у вістрі тріщини дозволяє пояснити явище міжшарової біфуркації і добре узгоджується із експериментальними даними.

1. D. J. Nicholls and J. P. Gallagher, "Determination of G_{Ic} in angle ply composites using a cantilever beam test method," *J. Reinforced Plastics and Composites*, No. 2, 2–17(1983).
2. P. Robinson and D. Q. Song, "A modified DCB specimen for Mode I of multidirectional laminates," *J. Composite Mater.*, **26**, No. 11, 1554–1577 (1992).
3. J. Whitney and L. M. Pinnel, "Characterization of interlaminar Mode II fracture using beam specimens," in: *Science and Technology of Composite Materials* (ECCM IV), Stuttgart (1990), pp. 865–868.
4. L. A. Carlsson, J. W. Gillepsie, Jr., and R. B. Pipes, "On the analysis and design of End-Notched Flexure (END) specimens for Mode II testing," *J. Composite Mater.*, **20**, 594–604 (1986).
5. J. Mall and P. Kochhar, "Finite-element analysis of end-notch flexure specimens," *J. Comp. Tech. Research*, **8**, No. 2, 54–57 (1986).
6. S. W. Tsai, *Theory of Composites Design*, Think Composites (1992).

7. *Ahmed Benyahia*, *Etude des Mecanismes de Délaminage sous l'Effet de Contrainte Complexes Générées Par des Sollicitation Simple d'Ouverture et de Cisaillement Dans les Stratifiés* $\pm\theta$, Thesis Université de Technologie de Compiègne, No. 1040 (1997).

8. A. Laksimi, A. Benyahia, M. Benzeggagh, and X. L. Gong, "Study of crack initiation and bifurcation mechanisms in a multidirectional laminate," *Composites Science and Technology*, **60**, 597–604 (2000).

9. D. Purslow, "Matrix fractography of fiber-epoxy," in: *Composites*, Royal Aircraft Establishment, Technical Report 86046 (1986).

Received 19. 09. 2001